

Impact of the QED corrections to the pion and kaon valence quark distribution functions: The valon model predictions

Akram Ghaffarian ,* Fatemeh Taghavi-Shahri ,[†]
Marzieh Mottaghizadeh ,[‡] and S. Shoeibi ,[§]

*Department of Physics, Faculty of Science,
Ferdowsi University of Mashhad,
Mashhad, Iran*

*akram.ghaffarian91@gmail.com

[†]taghavishahri@um.ac.ir

[‡]m_mottaghizadeh@yahoo.com

[§]samira.shoeibi1453@gmail.com

Received 13 September 2024

Revised 11 December 2024

Accepted 25 December 2024

Published 28 February 2025

This paper presents a study on the valence parton distribution functions (PDFs) of the pion and the kaon, which plays a crucial role in understanding the structure and interactions of hadrons. The study utilizes the valon model, which assumes that each hadron consists of two or three valence quarks, each carrying a fraction of the hadron's momentum. The valence PDFs of the pion and the kaon are calculated at a low initial scale and then evolved to higher scales using the QCD and the QED \otimes QCD Dokshitzer–Gribov–Lipatov–Altarelli–Parisi (DGLAP) evolution equations in Mellin space. A comparison is made between the obtained results and other theoretical and experimental data, demonstrating the predictive power of our approach for the pion and kaon PDFs in the context of the large hadron collider (LHC) as well. Furthermore, it is discovered that the pion valence PDFs moments agree with other phenomenological methods at different scales, indicating the consistency and reliability of our method.

Keywords: The valon model; Meson PDFs; QED corrections.

1. Introduction

Parton distribution functions (PDFs) for hadrons are essential for deciphering the dynamics of strong forces within the LHCs framework. They serve as a pivotal instrument in the colliders continuous quest to unravel the mysteries of the subatomic realm. The PDFs describe the probability of finding partons (quarks, gluons,

^{*}Corresponding author.

or even photons) carrying a certain fraction of the hadron's momentum. These PDFs serve as crucial ingredients for theoretical calculations and enable comparisons between predictions and experimental data. By obtaining reliable PDFs, we can make precise predictions about the behavior of the hadrons produced in collider experiments, facilitating a deeper understanding of their properties and interactions.

Experimental measurements of meson PDFs have been challenging due to their relatively low mass, making it difficult to separate their contributions from the more abundant background of protons and neutrons produced in colliders. However, significant advances have been made, and several experiments have successfully released data sensitive to the pion's PDFs using various techniques, including deep inelastic scattering^{1,2} and Drell–Yan processes.^{3–6} The internal structures of the pion and kaon, the lightest hadrons in nature, have been the subject of many recent studies.^{7–21} Understanding the pion's structure is crucial for studying other mesons and baryons, and it is necessary for developing a more complete picture of the strong nuclear force. Several theoretical models are used to study the pion's structure, including constituent quark models,²² chiral perturbation theory,²³ lattice QCD,²⁴ and also Dyson–Schwinger equations.²⁵ These models provide different approaches to understanding the structure and interactions of the pion and are often used in combination to obtain a more complete picture. The pion PDFs are important for a wide range of particle physics phenomena, including hadron colliders, dark matter searches, nucleon structures, and QCD calculations. Accurate measurements and theoretical calculations of the pion PDFs are necessary to make precise predictions and test the standard model. Deep inelastic scattering demonstrates that the hadron is a rather intricate entity made up of an endless array of quarks, antiquarks, and gluons. It is widely accepted that other strongly interacting particles also display a comparable internal structure. Nevertheless, under specific circumstances, hadrons function as though they are made up of three (or two) fundamental components. It makes sense to decompose a hadron into three (or two) constituent quarks, which carry the internal quantum numbers of the hadron. However, in deep inelastic scattering (DIS), a hadron appears to be composed of an essentially infinite number of quark–antiquark pairs and gluons, in addition to its valence quarks. One might identify the valence quark with a constituent quark, but this implies that the three (or two) quark model is a very rough approximation. To fully understand a hadron, one must also consider the quark–antiquark pairs and gluon degrees of freedom. This makes it challenging to comprehend why the three (or two) quark model of a hadron works so well in many situations. To reconcile this apparent contradiction, one can conceptualize a constituent quark as a quasi-particle possessing a complex internal structure. This structure comprises a valence quark enveloped by a sea of quark–antiquark pairs and gluons. This interpretation of the constituent quark is not new. R.C. Hwa expanded on this concept by introducing the more sophisticated valon model. The valon model was developed in the 1970s by Hwa to be an alternative to the quark model to investigate the nucleon structure.^{26–28} This model treats nucleons and mesons as bound states of three or two constituent quarks. In the

valon model, the nucleons and mesons are viewed as composite objects of smaller valons, which are themselves composite objects of other partons. According to the valon model, the hadronization process occurs in two stages. First, the valence quarks emit and absorb sea quarks, gluons, or even photons, leading to the development of a cloud which is referred to as **valons**. Then, these valons combine to form the resulting hadrons. There is a universal building block for every hadron called valon. The valon model frequently is used to study the nucleon unpolarized and polarized structure functions and also to study the light meson structure.^{29–33} Although this model is not new, new research have demonstrated that the introduced valon distribution functions for nucleons can be used to predict PDFs at energies available at the LHC too. The predicted PDFs and the results obtained from this model over a wide range of $x = [10^{-5}, 1]$ and $\mu^2 = [0.283, 10^8] \text{ GeV}^2$ are comparable to those from other phenomenological approaches. For more details, see Ref. 34.

From a theoretical perspective, M. Lavelle and D. McMullan demonstrated that it is possible to dress a QCD Lagrangian field to all orders in perturbation theory, thereby constructing a constituent quark consistent with color confinement.³⁵ In this framework, a valon is defined as a structured entity that emerges from the dressing of a valence quark with gluons and quark–antiquark pairs in QCD. So, a bound state of two or three “constituents-quark-like” valons can make a hadron, and these valons are the dressed valence quarks with their associated sea quarks and gluons (or even photons).

Experimental evidence for the existence of the valon has been obtained from measurements of the Nachtmann moments of the proton structure functions at Jefferson Laboratory.^{36,37} These measurements reveal a new scaling behavior that can be interpreted as a constituent form factor, consistent with elastic nucleon data. This suggests that the proton’s structure is influenced by elastic coupling of extended objects within the proton.

In this paper, we have a fresh look at the pion and kaon structures in the valon model. The main focus of this paper is to explore the valence quark’s PDFs inside the pion and kaon including the quantum electrodynamics (QED) corrections. The inclusion of QED corrections to the DGLAP evolution equations for hadron distribution functions is crucial for a comprehensive and precise understanding of hadron structure and its interactions at high-energy physics experiments. This research presents a forecast for the pion and kaon PDFs at the LHC’s high-energy scales, utilizing the valon phenomenological model as its framework. This paper is organized as follows. In Sec. 2, we review the valon model and its application to investigate the pion and kaon sub-structure. Next, in Sec. 3, we summarize the study’s key findings and present our conclusions regarding the implications of our results.

2. Method

Deep inelastic scattering (DIS) experiments probe the structure of hadrons at high momentum transfer. At high enough Q^2 , it is the structure of valons that is being probed, while at low enough μ^2 this structure cannot be resolved and

behaves as the valence quark and the hadron is viewed as the bound state of its valons. In this model, the structure-function of any hadron can be written as the convolution of the valon's distributions in the hadron with the structure-function of the valons

$$F_2^h(x, \mu^2) = \sum_{\text{valons}} \int_x^1 G_{\frac{\text{valon}}{h}}(y) F_2^{\text{valon}}\left(\frac{x}{y}, \mu^2\right) dy, \quad (1)$$

where summation runs over the number of valons in a particular hadron which is equal to the number of its valence quarks. $F_2^{\text{valon}}(z, Q^2)$ denotes the structure-function of a valon ($U, D, \bar{U}, \bar{D}, \dots$). $G_{\frac{\text{valon}}{h}}(y)$ is the probability of finding a valon carrying momentum fraction y of the hadron. The valon distribution functions are **not** related to the values of μ^2 , which means they are independent of the nature of the probe. As indicated by Eq. (1), the fundamental building blocks of the valon model can be constructed as follows:

- (1) Valons: The primary building blocks of the valon model are valons, which are clusters of partons (quarks and gluons or even photons). In the context of the proton, it is represented as a state of three valons (UUD), where U stands for up quarks and D for down quarks. In the pion (π^+), we also have two different valons, U and \bar{D} . To calculate the PDFs within a hadron, it is essential to know the valon distribution functions for that hadron.
- (2) Partons inside the valon: The model incorporates quarks and gluons (or even photon) as fundamental constituents of hadrons. Each valon can be thought of as a combination of these particles, and the model assumes that the proton consists of valence quarks, sea quarks, and gluons or photons associated to the valence quarks. To calculate the PDFs in the valon, we should solve the DGLAP evolution equations using appropriate initial inputs.

As we mentioned before, the valon model can investigate inside any hadron such as the proton, neutron, pion, and kaon. In the case of π^+ , it consists of two valons (or constituent quarks): U and \bar{D} . Similarly, a kaon, k^- , consists of two valons of S and \bar{U} . Figure 1 illustrates the structures of the pion (left) and kaon (right) mesons according to the valon model. As illustrated in the figure, a meson such as π^+ (or k^-), is composed of two valons. Each valon contains a single valence quark, and its associated sea partons and gluons or even photons.

The valence quark distributions inside the pion, say π^+ , can be written as follows:

$$\begin{aligned} u_{\text{valence}\pi^+}(x, \mu^2) &= \int_x^1 G_{\frac{U}{\pi^+}}(y) u_{\frac{\text{valence}}{U}}\left(\frac{x}{y}, \mu^2\right) \frac{dy}{y}, \\ \bar{d}_{\text{valence}\pi^+}(x, \mu^2) &= \int_x^1 G_{\frac{\bar{D}}{\pi^+}}(y) \bar{d}_{\frac{\text{valence}}{\bar{D}}}\left(\frac{x}{y}, \mu^2\right) \frac{dy}{y}. \end{aligned} \quad (2)$$

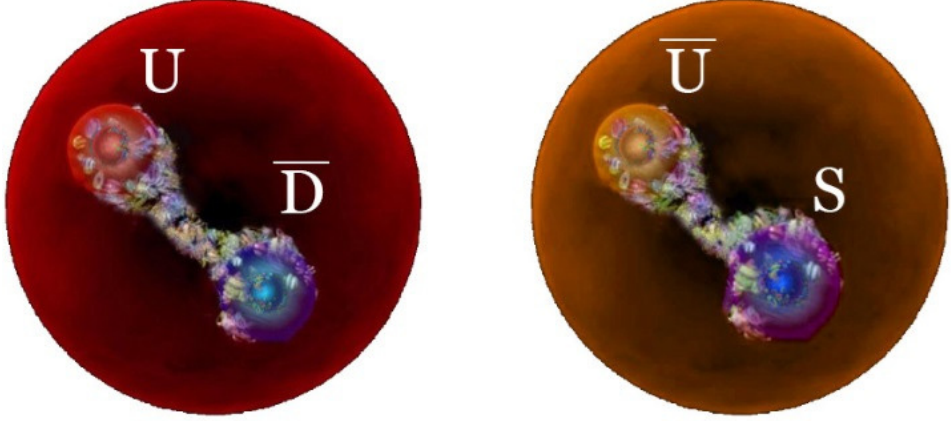


Fig. 1. A schematic picture of the π^+ (left) and k^- (right) structures in the valon model.

Here, subscripts U and \bar{D} denote the two valons in π^+ . In this equation, $u_{\text{valence}}\left(\frac{x}{y}, \mu^2\right)$ and $\bar{d}_{\text{valence}}\left(\frac{x}{y}, \mu^2\right)$ are the valence quark distributions inside the pion that can be calculated from solving the well-known Dokshitzer–Gribov–Lipatov–Altarelli–Parisi (DGLAP) evolution equations^{38–41} inside valons using the suitable initial inputs inside valon. Fortunately, the solution of the DGLAP evolution equations is known in Mellin space in QCD^{42–44} or with QED corrections in QED \otimes QCD DGLAP evolution equations.⁴⁵ Furthermore, these solutions have been skillfully utilized to precisely determine the PDFs within the proton, incorporating QED corrections.³⁴ According to our previous work,⁴⁵ the singlet PDFs, $f_i(x, \mu^2)$, obey the QED \otimes QCD DGLAP evolution equations^{46,47} in x space, as

$$\frac{\partial}{\partial \log \mu^2} \begin{pmatrix} f_1 \\ f_2 \\ f_3 \\ f_4 \end{pmatrix} = \begin{pmatrix} P_{11} & P_{12} & P_{13} & P_{14} \\ P_{21} & P_{22} & P_{23} & P_{24} \\ P_{31} & P_{32} & P_{33} & P_{34} \\ P_{41} & P_{42} & P_{43} & P_{44} \end{pmatrix} \otimes \begin{pmatrix} f_1 \\ f_2 \\ f_3 \\ f_4 \end{pmatrix}, \quad (3)$$

and the QED \otimes QCD DGLAP evolution equations for the nonsinglet PDFs are as follows:

$$\frac{\partial f_i}{\partial \log \mu^2} = P_{ii} \otimes f_i, \quad i = 5, \dots, 9, \quad (4)$$

where P_{ij} and P_{ii} are the splitting functions and represented in Ref. 45, and \otimes denotes the convolution integral

$$f \otimes g = \int_x^1 \frac{dy}{y} f(y) g\left(\frac{x}{y}\right). \quad (5)$$

In Ref. 45, we employed a PDF framework for the QED \otimes QCD DGLAP evolution equations, characterized by the following singlet and nonsinglet PDF combinations:

$$q^{SG} : \begin{pmatrix} f_1 = \Delta = \\ u + \bar{u} + c + \bar{c} - d - \bar{d} - s - \bar{s} - b - \bar{b} \\ f_2 = \Sigma = \\ u + \bar{u} + c + \bar{c} + d + \bar{d} + s + \bar{s} + b + \bar{b} \\ f_3 = g \\ f_4 = \gamma \end{pmatrix}, \quad (6)$$

$$q^{NS} : \begin{pmatrix} f_5 = d_v = d - \bar{d} \\ f_6 = u_v = u - \bar{u} \\ f_7 = \Delta_{ds} = d + \bar{d} - s - \bar{s} \\ f_8 = \Delta_{uc} = u + \bar{u} - c - \bar{c} \\ f_9 = \Delta_{sb} = s + \bar{s} - b - \bar{b} \end{pmatrix}, \quad (7)$$

and we also assume the symmetry between quarks and antiquarks distributions. Then, we have $s = \bar{s}$, $c = \bar{c}$ and $b = \bar{b}$.

To investigate the PDFs inside pion based on the Eq. (2), we need the valon distribution functions inside this meson: $G_{\frac{u}{\pi^+}}(y)$ and $G_{\frac{\bar{d}}{\pi^+}}(y)$. Following Refs. 30 and 31, the valon distribution functions inside any hadron obey the general functional form:

$$G_{valon/hadron}(y) = \frac{1}{B(\mu + 1, \nu + 1)} y^\mu (1 - y)^\nu, \quad (8)$$

where $B(\mu + 1, \nu + 1)$ is the known beta function. Parameters μ and ν should be calculated from experimental data for any hadron. Actually, the key aspect of employing the valon model is that, although phenomenological groups rely on experimental data to establish many parameters incorporated in the initial PDFs, the valon model utilizes experimental data to ascertain only a few parameters of the valon distribution functions. Interestingly, these valon distribution functions are not μ^2 dependent. Once determined for each hadron, it can be used to calculate the hadron's PDFs at any value of μ^2 . Therefore, to study the PDFs inside the pion (kaon or any meson), we must solve the DGLAP evolution equations in the valon using suitable initial inputs. Then, to calculate the pion PDFs as an example, the convolution of the valon distribution functions of the pion with those PDFs inside valons leads us to the PDFs inside pion. The valon distribution functions also satisfy the following number and momentum sum rules

$$\begin{aligned} \int_0^1 G_{\frac{u}{hadron}}(y) dy &= 1 \\ \sum_{valons} \int_0^1 y G_{\frac{u}{hadron}}(y) dy &= 1. \end{aligned} \quad (9)$$

In this paper, we want to study the valence quark distribution functions inside the pion (π^+) and kaon (k^+) first in QCD with the DGLAP evolution equations and then, with the QED corrections using the QED \otimes QCD DGLAP evolution equations. The initial step involves computing the PDFs within each valon through the utilization of the DGLAP evolution equations. To solve the DGLAP evolution equations, we need initial input densities in the valons. We work in the \overline{MS} scheme with $\Lambda_{QCD} = 0.33 \text{ GeV}$ ($\Lambda_{QCD} = 0.22 \text{ GeV}$) in initial scale of $\mu_0^2 = 0.283 \text{ GeV}^2$ for three (five) active flavors. At such a low initial scale of μ_0^2 , the mesons can be considered as a bound state of two valence quarks that carry all of the meson's momenta. Therefore, at this scale of μ_0^2 , there is one valence quark in each valon and this valence quark carries all of the valon's momenta. So the initial input densities in the valon model can be considered as $\delta(z - 1)$ for valence quarks and zero for sea quarks and gluons or even photon distributions, respectively. Then, the initial input densities in Mellin space are one for the valence PDFs inside valons, and zero for other parton densities. The next step in determining the PDFs of pion and kaon involves finding the distribution functions of the valons present inside these mesons. We use the valon distributions introduced in Refs. 30 and 31 for the pion (π^+).

$$G_{\frac{U}{\pi^+}} = G_{\frac{\bar{D}}{\pi^+}} = 1.071(1 - y)^{0.06}y^{0.01}. \quad (10)$$

To calculate the PDFs inside kaon (k^+), we follow the same procedure, but now the distribution of the valons in the kaon is given as Refs. 30 and 31.

$$G_U^{k^+}(y) = 1.4768y^{0.13}(1 - y)^{0.28}, \quad G_{\bar{S}}^{k^+}(y) = 1.4768y^{0.28}(1 - y)^{0.13}. \quad (11)$$

These Valon distributions are plotted in Fig. 2. One can check that these valon distributions almost satisfy Eq. (9).

Finally, the most important parameters involved in the valon model can be summarized as follows: Momentum fraction (z): The model includes parameters related to the momentum fraction of quarks within the valons, which are crucial for the initial distribution functions. The valon model employs straightforward initial quark distribution functions, which are $\delta(z - 1)$ for the valence quarks and zero for other partons at a low initial scale of $\mu_0^2 = 0.283, \text{ GeV}^2$. The value of μ_0^2 corresponds to a distance of 0.36 fm, which is roughly equivalent to or slightly less than the radius of a constituent quark (CQ) or valon. It can be contended that such distances are likely too extensive for a significant pure perturbative analysis. Specifically, μ_0 represents the leading-order effective value at which the hadron can be considered as consisting of only three (for baryons) or two (for mesons) CQs. Our analysis confirms that as μ^2 approaches μ_0^2 , the quark moments approach unity, while the gluon moments approach zero. This initial low μ_0^2 led to a good description of the proton PDFs in the valon model as well. For more details, see Ref. 34.

Number of flavors and Λ_{QCD} are important in the valon model to solve the DGLAP evolution equations inside valon and also for calculating the valon

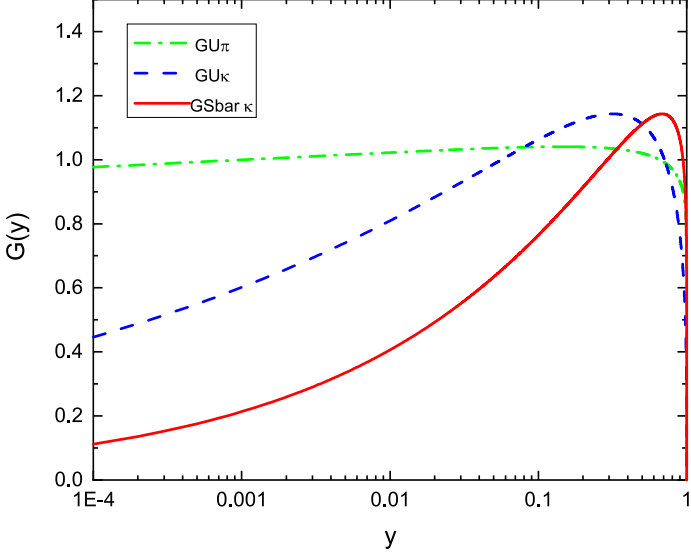


Fig. 2. The valon distributions of the π^+ ($G_{\frac{U}{\pi^+}}$), and k^+ ($G_U^{k^+}(y)$, $G_S^{k^+}(y)$).

distribution functions using the experimental data. However, in this work, we used the valon distribution functions in the pion and kaon as proposed in Refs. 30 and 31. So, to calculate the valence quark PDFs inside the pion (kaon):

- Solve the DGLAP evolution equations within the valon using appropriate initial inputs: $\delta(z - 1)$ for the valence quark inside the valon and zero for other parton distributions.
- By utilizing the valon distribution functions for the pion (kaon) and applying the convolution integral in Eq. (2), the valence quark PDFs are calculated within the pion (kaon).

3. Results and Discussion

In this section, we present the outcomes acquired for the pion and kaon PDFs, with and without QED corrections to the DGLAP evolution equations. Initially, we employ the QCD DGLAP evolution equation with three symmetric flavors, denoted as $n_f = 3$, in the Fixed Flavor Number Scheme (FFNS). Moreover, we utilize a value of $\Lambda_{QCD} = 0.33 \text{ GeV}$ to compute the PDFs within the pion and kaon, employing the previously described valon model (Scenario A). This QCD DGLAP evolution equations are then run with $n_f = 5$ and $\Lambda_{QCD} = 0.22 \text{ GeV}$ to calculate the PDFs at very high energy without including the QED corrections (Scenario B). Then, we proceed to the next step, where we adopt the QED \otimes QCD DGLAP evolution equation to the usage of five symmetric flavors, along with $\Lambda_{QCD} = 0.22 \text{ GeV}$, in order to examine the influence of QED corrections on the previous outcomes

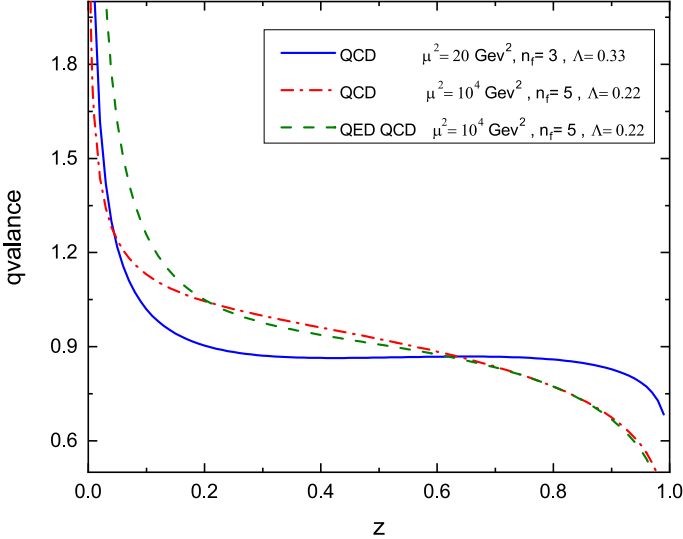


Fig. 3. Valence quark distributions within each valon are calculated at $\mu^2 = 20 \text{ GeV}^2$ (scenario A), and at $\mu^2 = 10^4 \text{ GeV}^2$, using the QCD DGLAP evolution equations (scenario B), as well as the combined QED \otimes QCD DGLAP evolution equations (scenario C).

(Scenario C). The results show that including the QED corrections to the DGLAP evolution equations reduces the contribution of the valence quarks inside the pion and kaon.

In Fig. 3, we show the valence quark distributions inside each valon as a function of $z = \frac{x}{y}$, at $\mu^2 = 20 \text{ GeV}^2$ (Scenario A), and at $\mu^2 = 10^4 \text{ GeV}^2$ (Scenario B), using the QCD DGLAP evolution equations as well as the combined QED \otimes QCD DGLAP evolution equations for $\mu^2 = 10^4 \text{ GeV}^2$ (Scenario C).

Using the valon distributions of the pion introduced in Eq. (10), we calculate the valence quark distributions within this meson using Eq. (2). The results, depicted in Fig. 4, were then compared with those from the E615 experimental data⁶ and various phenomenological models, including JAM,¹⁴ xFitter,¹⁶ and BLFQ.¹⁵ Our findings show a nice agreement with these models. In the following, we calculate the valence quark distributions in the pion at $\mu^2 = 10^4 \text{ GeV}^2$ in two scenarios B and C: Using only the QCD DGLAP evolution equations and using the combined QED \otimes QCD DGLAP evolution equations to investigate the influence of the QED correction on the valence quarks distributions in the pion. The results presented in Fig. 5 indicate that applying of the QED corrections leads to a slight reduction in the distribution functions of valence quark distributions inside pion at very high energies.

To examine the impact of QED corrections on the kaon (k^+) valence quark distributions, we employed the same algorithm. The results are illustrated in Figs. 6 and 7. Figure 6 presents the valon model prediction for the valence quark distribution functions in the kaon at $\mu^2 = 20 \text{ GeV}^2$ in scenario A, compared with those from BLFQ-NJL. Figure 7 demonstrates that incorporating QED corrections into the

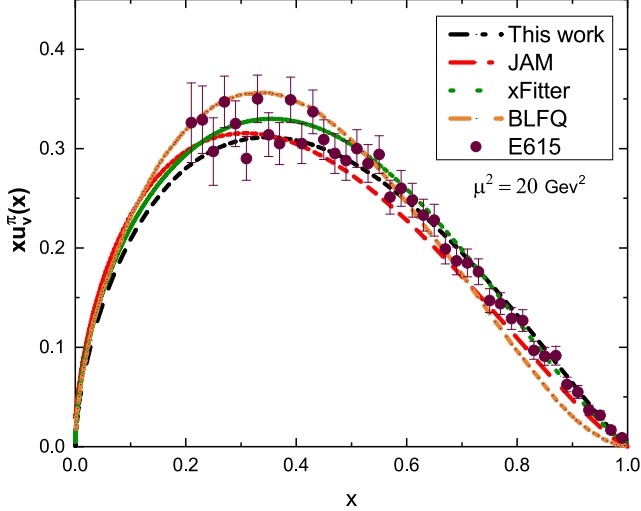


Fig. 4. Valence quark distributions in the valon model at $\mu^2 = 20 \text{ GeV}^2$ using the QCD DGLAP evolution equations in scenario A, and comparison with phenomenological models and E615 experimental data.⁶

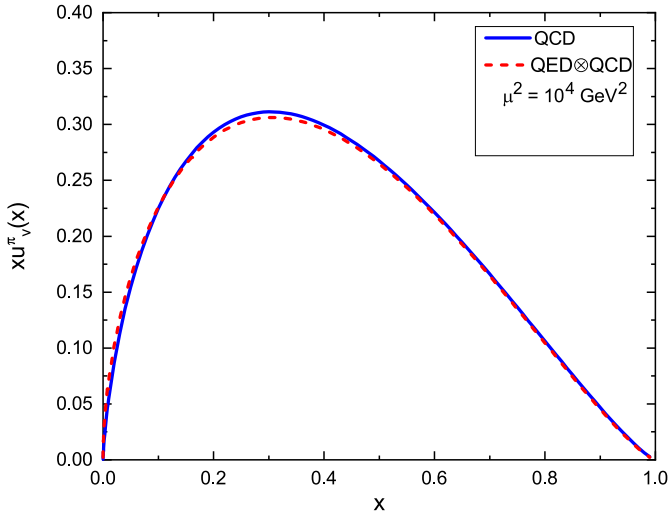


Fig. 5. (Color online) Valence quark distributions in the valon model at $\mu^2 = 10^4 \text{ GeV}^2$ with the QCD DGLAP evolution equations in scenario B (blue), and with the QED \otimes QCD DGLAP evolution equations in scenario C (dashed red).

DGLAP evolution equation significantly reduces the valence quark distributions at the high energy of $\mu^2 = 10^4 \text{ GeV}^2$. The two figures demonstrate that, as the energy increases from $\mu^2 = 20 \text{ GeV}^2$ to $\mu^2 = 10^4 \text{ GeV}^2$, the valence quark distributions decrease when using the QCD DGLAP evolution equations. This reduction becomes even more significant when the QED \otimes QCD DGLAP equations are employed.

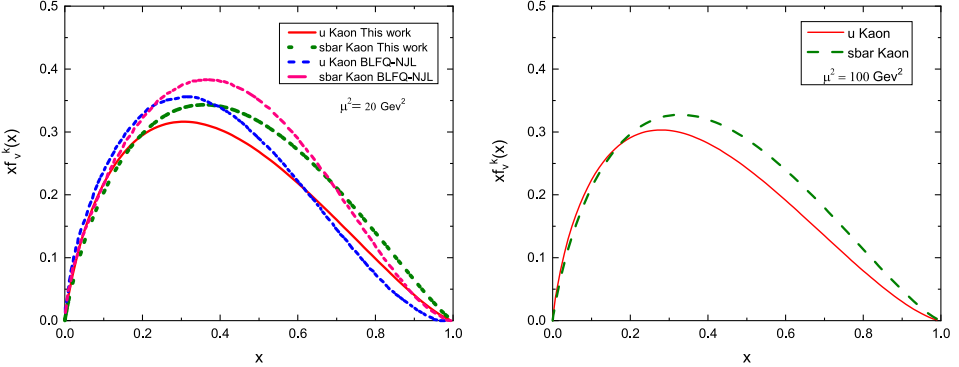


Fig. 6. Valon model prediction for the valence quark distribution functions in the kaon at $\mu^2 = 20 \text{ GeV}^2$ and $\mu^2 = 100 \text{ GeV}^2$ in scenario A, and comparison with those from BLFQ-NJL.

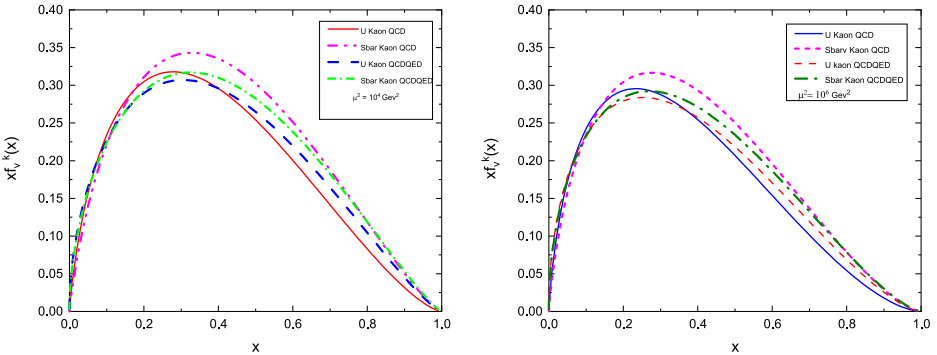


Fig. 7. Valence quark distributions in the kaon at $\mu^2 = 10^4 \text{ GeV}^2$ (Left) and $\mu^2 = 10^6 \text{ GeV}^2$ (Right) with the QCD DGLAP evolution equations in scenario B, and with the QED \otimes QCD DGLAP evolution equations in scenario C.

We also compare our results for $\frac{x u_v^k}{x u_v^\pi}$ with experimental data from⁴ at $\mu^2 = 20 \text{ GeV}^2$ in Fig. 8. The lowest four moments of the valence quark PDFs in the pion and kaon, as predicted by the valon model using the QCD DGLAP evolution equations in scenario A, and its comparison with the results obtained from other models at different scales are shown in Tables 1 and 2, respectively. All results show an acceptable agreement with them. Finally, in Tables 3 and 4, we present the prediction of the valon model for the lowest four moments of the valence quark PDFs in the pion and kaon using the QED \otimes QCD DGLAP evolution equation in scenario C, at different high-value scales of 10^4 GeV^2 , 10^6 GeV^2 and 10^8 GeV^2 . The data presented in the tables indicate that, at each energy level, the values of the higher moments are smaller. Additionally, the moments of the valence quark distributions diminish as the energy increases.

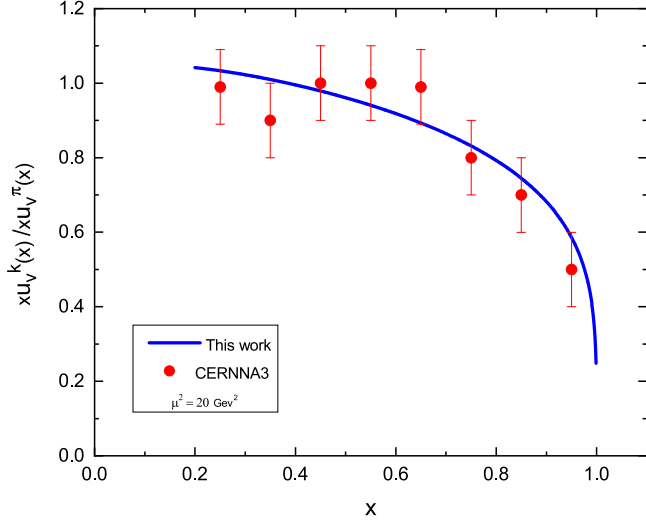


Fig. 8. The valence quark distributions ratio in pion and kaon at $\mu^2 = 20 \text{ (GeV}^2)$ in scenario A. Experimental data are from Ref. 4.

Table 1. The lowest four moments of the valence quark PDF in the pion in scenario A, as predicted by the valon model using the QCD DGLAP evolution equations, and its comparison with the results obtained from the global fit, lattice QCD, BLFQ, and phenomenological models at different scales.

Model	μ^2 (GeV 2)	$\langle x \rangle$	$\langle x^2 \rangle$	$\langle x^3 \rangle$	$\langle x^4 \rangle$
DSE-RL (2018) ⁷	1.69	0.268	0.125	0.076	0.054
JAM global fit (2018) ¹⁴		0.268	0.127	0.074	0.048
BLFQ-NJL (2020) ¹⁵	$0.271_{-0.020}^{+0.020}$	$0.124_{-0.014}^{+0.014}$	$0.069_{-0.009}^{+0.009}$	$0.044_{-0.007}^{+0.007}$	
This work	0.263	0.128	0.076	0.051	
Sutton (1992) ⁸	4	0.24 ± 0.01	0.10 ± 0.01	0.058 ± 0.004	
Hecht (2001) ⁹		0.24	0.098	0.049	
Chen (2016) ¹⁰		0.26	0.11	0.052	
BSE (2019) ¹¹		0.24 ± 0.02			
DESY (2016) [lattice QCD] ¹²		0.214 ± 0.015			
ETM (2018) [lattice QCD] ¹³		0.207 ± 0.011	0.163 ± 0.033		
JAM global fit (2018) ¹⁴		0.245 ± 0.005	0.108 ± 0.003	0.061	
BLFQ-NJL (2020) ¹⁵		$0.245_{-0.018}^{+0.018}$	$0.106_{-0.012}^{+0.012}$	$0.057_{-0.008}^{+0.008}$	$0.035_{-0.005}^{+0.005}$
xFitter ¹⁶		0.24	0.11	0.063	
This work		0.236	0.109	0.062	0.040
Detmold (2003) [lattice QCD] ¹⁷	5.76	0.24 ± 0.01	0.09 ± 0.03	0.043 ± 0.015	
BLFQ-NJL (2020) ¹⁵		$0.236_{-0.018}^{+0.018}$	$0.101_{-0.011}^{+0.011}$	$0.054_{-0.007}^{+0.007}$	$0.032_{-0.005}^{+0.005}$
This work		0.228	0.103	0.058	0.037
Watanabe (2018) ¹⁸	27	0.23	0.094	0.048	
Nam (2012) ¹⁹		$0.214_{-0.030}^{+0.016}$	$0.087_{-0.019}^{+0.010}$	$0.044_{-0.011}^{+0.006}$	$0.026_{-0.008}^{+0.004}$
Wijesooriya (2005) ²⁰		0.217 ± 0.011	0.087 ± 0.005	0.045 ± 0.003	
BLFQ-NJL (2020) ¹⁵		$0.210_{-0.016}^{+0.016}$	$0.084_{-0.009}^{+0.009}$	$0.043_{-0.006}^{+0.006}$	$0.025_{-0.004}^{+0.004}$
This work		0.203	0.086	0.046	0.029
Sutton (1992) ⁸	49	0.200 ± 0.015	0.080 ± 0.007		
BLFQ-NJL(2020) ¹⁵		$0.202_{-0.015}^{+0.015}$	$0.079_{-0.009}^{+0.009}$	$0.040_{-0.005}^{+0.005}$	$0.023_{-0.003}^{+0.003}$
This work		0.196	0.081	0.043	0.026

Table 2. Lowest four moments of valence quark distributions in the kaon based on the valon model in scenario A, and comparison other phenomenological results.

Flavor	Model	μ^2 (GeV 2)	$\langle x \rangle$	$\langle x^2 \rangle$	$\langle x^3 \rangle$	$\langle x^4 \rangle$
s^K	BLFQ-NJL	1	$0.320^{+0.024}_{-0.024}$	$0.158^{+0.018}_{-0.017}$	$0.093^{+0.013}_{-0.012}$	$0.061^{+0.010}_{-0.009}$
	This work		0.277	0.135	0.080	0.053
u^K	BLFQ-NJL		$0.282^{+0.021}_{-0.021}$	$0.128^{+0.014}_{-0.014}$	$0.071^{+0.010}_{-0.010}$	$0.044^{+0.007}_{-0.007}$
	This work		0.314	0.164	0.0102	0.070
s^K	BLFQ-NJL	4	$0.266^{+0.020}_{-0.020}$	$0.119^{+0.013}_{-0.013}$	$0.066^{+0.009}_{-0.009}$	$0.041^{+0.006}_{-0.006}$
	This work		0.257	0.121	0.070	0.045
u^K	BLFQ-NJL		$0.235^{+0.017}_{-0.018}$	$0.097^{+0.011}_{-0.011}$	$0.050^{+0.007}_{-0.007}$	$0.030^{+0.005}_{-0.005}$
	This work		0.227	0.100	0.055	0.034
s^K	BLFQ-NJL	16	$0.237^{+0.018}_{-0.018}$	$0.100^{+0.011}_{-0.011}$	$0.052^{+0.007}_{-0.007}$	$0.031^{+0.005}_{-0.005}$
	This work		0.229	0.101	0.056	0.035
u^K	BLFQ-NJL		$0.209^{+0.015}_{-0.016}$	$0.081^{+0.009}_{-0.009}$	$0.040^{+0.006}_{-0.005}$	$0.023^{+0.004}_{-0.003}$
	This work		0.202	0.083	0.044	0.026
s^K	Chen (2016) ¹⁰	27	0.36	0.17	0.092	
	Watanabe (2018) ²¹		0.24	0.096	0.049	
	BLFQ-NJL ¹⁵		$0.228^{+0.017}_{-0.017}$	$0.094^{+0.010}_{-0.010}$	$0.049^{+0.007}_{-0.007}$	$0.029^{+0.005}_{-0.004}$
	This work		0.221	0.096	0.052	0.032
u^K	Chen (2016) ¹⁰		0.28	0.11	0.048	
	Watanabe (2018) ²¹		0.23	0.091	0.045	
	BLFQ-NJL ¹⁵		$0.201^{+0.015}_{-0.015}$	$0.077^{+0.009}_{-0.008}$	$0.037^{+0.005}_{-0.005}$	$0.021^{+0.003}_{-0.003}$
	This work		0.195	0.079	0.041	0.024

Table 3. Prediction of the valon model for the lowest four moments of the valence quark PDFs in the pion using the QED \otimes QCD DGLAP evolution equations in scenario C, at different high value scales with $n_f = 5$ and $\Lambda = 0.22\text{ GeV}$.

Flavor	μ^2 (GeV 2)	$\langle x \rangle$	$\langle x^2 \rangle$	$\langle x^3 \rangle$	$\langle x^4 \rangle$
$u_v^\pi (= d_v^\pi)$	10^4	0.197	0.0797	0.042	0.026
	10^6	0.171	0.064	0.032	0.019
	10^8	0.153	0.054	0.026	0.015

Table 4. Prediction of the valon model for the lowest four moments of the valence quark PDFs in the kaon using the QED \otimes QCD DGLAP evolution equations in scenario C, and at different high-value scales.

Flavor	μ^2 (GeV 2)	$\langle x \rangle$	$\langle x^2 \rangle$	$\langle x^3 \rangle$	$\langle x^4 \rangle$
s^K	10^4	0.214	0.089	0.047	0.029
	10^6	0.187	0.071	0.036	0.021
	10^8	0.167	0.060	0.029	0.016
u^K	10^4	0.189	0.073	0.037	0.022
	10^6	0.164	0.059	0.028	0.016
	10^8	0.147	0.049	0.023	0.012

4. Summary and Conclusions

In our study, we focused on calculating the valence PDFs of the pion and the kaon using the valon model. This model provides a framework for understanding the internal structure of these mesons in terms of their CQs and gluons. Additionally, we examined the impact of QED corrections on the valence PDFs, which are essential for achieving more accurate theoretical predictions.

Our results showed that the moments of the valence PDFs for both the pion and the kaon are consistent with several phenomenological models. This agreement across a range of energy scales reinforces the validity of the valon model as a robust phenomenological tool for describing the partonic structure of the pion and the kaon.

The findings from our study contribute to the broader understanding of the fundamental properties of pions and kaons. By providing a detailed analysis of their valence PDFs, we offer insights that could influence future theoretical research in particle physics. Our work highlights the importance of considering QED corrections and suggests that further precision can be achieved by incorporating higher-order corrections.

Looking ahead, there are several promising directions for future research. One avenue is to compute the PDFs for other components, such as the distributions of sea quarks and gluons, and also photons within the pion and kaon. Additionally, incorporating higher-order QED corrections could further refine our predictions and enhance the accuracy of the valon model. These efforts will continue to advance our understanding of meson structure and the fundamental interactions governing particle physics.

Acknowledgments

The authors acknowledge the Ferdowsi University of Mashhad for the provided facilities to do this project. This work is supported by the Ferdowsi University of Mashhad under grant number 3/59020(1401/11/17).

ORCID

Akram Ghaffarian  <https://orcid.org/0009-0006-7224-2713>
Fateme Taghavi-Shahri  <https://orcid.org/0000-0002-7242-5564>
Marzieh Mottaghizadeh  <https://orcid.org/0000-0001-6803-2533>
S. Shoeibi  <https://orcid.org/0000-0001-8910-0160>

References

1. ZEUS Collab. (S. Chekanov *et al.*) *Nucl. Phys. B* **637**, 3 (2002).
2. The H1 Collab. (F. D. Aaron *et al.*) *Eur. Phys. J. C* **68**, 381 (2010).
3. J. Badier *et al.* *Phys. Lett. B* **93**, 354 (1980).
4. NA3 Collab. (J. Badier *et al.*) *Z. Phys. C* **18**, 281 (1983).
5. NA10 Collab. (B. Betev *et al.*) *Z. Phys. C* **28**, 9 (1985).
6. J. S. Conway *et al.* *Phys. Rev. D* **39**, 92 (1989).

7. K. D. Bednar, I. C. Cloët and P. C. Tandy, *Phys. Rev. Lett.* **124**(4), 042002 (2020).
8. P. J. Sutton, A. D. Martin, R. G. Roberts and W. J. Stirling, *Phys. Rev. D* **45**, 2349 (1992).
9. M. B. Hecht, C. D. Roberts and S. M. Schmidt, *Phys. Rev. C* **63**, 025213 (2001).
10. C. Chen, L. Chang, C. D. Roberts, S. Wan and H. S. Zong, *Phys. Rev. D* **93**, 074021 (2016), <https://doi.org/10.1103/PhysRevD.93.074021>.
11. M. Ding, K. Raya, D. Binosi, L. Chang, C. D. Roberts and S. M. Schmidt, *Phys. Rev. D* **101**, 054014 (2020).
12. A. Abdel-Rehim *et al.* *Phys. Rev. D* **92**, 114513 (2015).
13. M. Oehm, C. Alexandrou, M. Constantinou, K. Jansen, G. Koutsou, B. Kostrzewa, F. Steffens, C. Urbach and S. Zafeiropoulos, *Phys. Rev. D* **99**, 014508 (2019).
14. P. C. Barry, N. Sato, W. Melnitchouk and C. R. Ji, *Phys. Rev. Lett.* **121**, 152001 (2018).
15. J. Lan, C. Mondal, S. Jia, X. Zhao and J. P. Vary, *Phys. Rev. D* **101**, 034024 (2020).
16. I. Novikov *et al.* *Phys. Rev. D* **102**, 014040 (2020).
17. W. Detmold, W. Melnitchouk and A. W. Thomas, *Phys. Rev. D* **68**, 034025 (2003).
18. A. Watanabe, T. Sawada and C. W. Kao, *Phys. Rev. D* **97**, 074015 (2018).
19. S. I. Nam, *Phys. Rev. D* **86**, 074005 (2012).
20. K. Wijesooriya, P. E. Reimer and R. J. Holt, *Phys. Rev. C* **72**, 065203 (2005).
21. A. Watanabe, T. Sawada and C. W. Kao, *Nucl. Part. Phys. Proc.* **300–302**, 121 (2018).
22. G. Altarelli, S. Petrarca and F. Rapuano, *Phys. Lett. B* **373**, 200 (1996).
23. E. Ruiz Arriola, https://doi.org/10.1142/9789812799708_0005, arXiv:hep-ph/0107087 [hep-ph] (2001).
24. J. H. Zhang, J. W. Chen, L. Jin, H. W. Lin, A. Schäfer and Y. Zhao, *Phys. Rev. D* **100**, 034505 (2019).
25. C. Shi, C. Mezrag and H. S. Zong, *Phys. Rev. D* **98**, 054029 (2018).
26. R. C. Hwa, *Phys. Rev. D* **22**, 759 (1980).
27. R. C. Hwa, *Phys. Rev. D* **51**, 85 (1995).
28. R. C. Hwa and C. B. Yang, *Phys. Rev. C* **66**, 025204 (2002).
29. F. Arash and A. N. Khorramian, *Phys. Rev. C* **67**, 045201 (2003).
30. F. Arash, *Phys. Lett. B* **557**, 38 (2003).
31. F. Arash, *Phys. Rev. D* **69**, 054024 (2004).
32. Z. Alizadeh Yazdi, F. Taghavi-Shahri, F. Arash and M. E. Zomorrodian, *Phys. Rev. C* **89**, 055201 (2014).
33. F. Arash and F. Taghavi-Shahri, *J. High Energy Phys.* **07**, 071 (2007).
34. M. Mottaghizadeh, F. Taghavi Shahri and P. Eslami, *Phys. Rev. D* **96**, 074001 (2017).
35. M. Lavelle and D. McMullan, *Phys. Rep.* **279**, 1 (1997).
36. M. Okumura and Y. Okumura, *Prog. Theor. Phys.* **63**, 217 (1980).
37. CLAS Collab. (M. Osipenko *et al.*) *Phys. Rev. D* **67**, 092001 (2003).
38. G. Altarelli and G. Parisi, *Nucl. Phys. B* **126**, 298 (1977).
39. Y. L. Dokshitzer, *Sov. Phys. JETP* **46**, 641 (1977) [*Zh. Eksp. Teor. Fiz.* **73**, 1216 (1977)].
40. V. N. Gribov and L. N. Lipatov, *Sov. J. Nucl. Phys.* **15**, 438 (1972) [*Yad. Fiz.* **15**, 781 (1972)].
41. L. N. Lipatov, *Sov. J. Nucl. Phys.* **20**, 94 (1975) [*Yad. Fiz.* **20**, 181 (1974)].
42. J. Blumlein, S. Riemersma, W. L. van Neerven and A. Vogt, *Nucl. Phys. B Proc. Suppl.* **51**, 97 (1996).
43. S. Moch, J. A. M. Vermaasen and A. Vogt, *Nucl. Phys. B* **688**, 101 (2004).
44. A. Vogt, *Comput. Phys. Commun.* **170**, 65 (2005).
45. M. Mottaghizadeh, F. Taghavi Shahri and P. Eslami, *Phys. Lett. B* **773**, 375 (2017).
46. S. Carrazza, <https://doi.org/10.48550/arXiv.1509.00209>, arXiv:1509.00209 [hep-ph] (2015).
47. M. Roth and S. Weinzierl, *Phys. Lett. B* **590**, 190 (2004).